Phase field dynamic modelling of shape memory alloys based on isogeometric analysis

Dhote, R., Gomez, H., Melnik, R., Zu, J.

Phase Field Dynamic Modelling of Shape Memory Alloys Based on Isogeometric Analysis

Rakesh Dhote[1,3,a], Hector Gomez[2], Roderick Melnik[3,4], and Jean Zu[1]

[1]Department of Mechanical & Industrial Engineering, University of Toronto, Canada

[2]Department of Applied Mathematics, University of A Coruña, Spain

[3]M²NeT Laboratory, Wilfrid Laurier University, Waterloo, Canada
[4]Ikerbasque, BFS and BCAM, Spain
[a]rakesh.dhote@utoronto.ca, * Corresponding author

Keywords: Isogeometric analysis, martensitic transformations, phase-field model, Ginzburg-Landau theory, nonlinear thermo-elasticity.

Abstract. Shape Memory Alloys (SMAs) exhibit complex behaviors as a result of their constituent phases and microstructure evolution. In this paper, we focus on the numerical simulations of microstructure evolution in SMAs using a phase-field model for the two dimensional square- to- rectangular martensitic phase transformations. The phase-field model, based on the Ginzburg-Landau theory, has strong non-linearity, thermo-mechanical coupling, and higher-order differential terms and presents substantial challenges for numerical simulations. The isogeometric analysis, developed in this paper using the rich NURBS basis functions, offers several advantages in solving such complex problems with higher-order partial differential equations as the problem at hand. To our best knowledge, we report here for the first time the use of the new method in the study of microstructure evolution in SMAs. The numerical experiments of microstructure evolution have been carried out on the FePd SMA specimen. The results are in good agreement with those previously reported in the literature.

Introduction

Shape Memory Alloys have attracted considerable attention of physicists, engineers and mathematicians due to their interesting properties of shape recovery, as well as their temperature dependent non-linear hysteretic behavior. These properties are result of atomic reorientations known as martensitic phase transformations (PTs). The martensitic PT is a mechanically or thermally induced reversible PT from high-symmetry arrangements to low-symmetry arrangements of atoms with displacements less than an atomic distance. The cumulation of displacements over several atomic layers yields into a macroscopic shape change in the specimen. The dynamics of PT, thermal and mechanical loadings give rise to the two unique characteristics of SMAs namely, shape memory effect and superelasticity. These characteristics have been extensively studied and applied successfully in commercial applications [1].

Over the last decade, many research efforts in SMAs have been focused on developing dynamic mathematical models to describe non-linear hysteretic temperature-dependent behaviors of these materials [2, 4, 5, 11]. Specifically, the phase-field (PF) models have emerged as a powerful computational tool for modeling microstructures and their mechanical properties [3, 4, 5]. The PF model maintains different phases in a domain by minimizing the free energy and by introducing a smoothly varying interface, a domain wall. The inclusion of domain wall in a system results in the fourth-order partial differential equations (PDEs) in space. Numerical methodologies such as finite difference, finite volume, and spectral methods have been traditionally used in this field for solving higher order PDEs [5, 6]. These methodologies have been mostly applied to simple geometries. However for the real world SMA applications [1], a more geometrically flexible technology needs to be utilized. In this situation, one can resort to the finite element method, which has wide applicability across engineering disciplines to simulate physics with geometric flexibility. The finite element method also
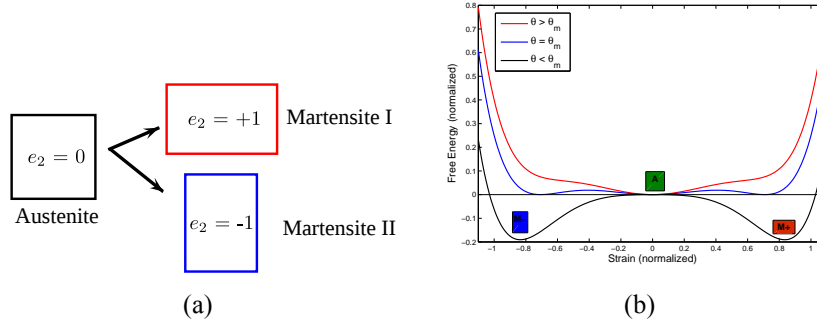
Fig. 1: Schematic showing (a) square-to-rectangular PT, and (b) the free energy and temperature dependent phases.

offers flexibility in treating complex boundary conditions and second order PDEs, where the continuity requirements on the trial functions can be reduced to global $\mathscr{C}^0$-continuity. However, for the fourth-order PDEs, the basis functions need to be piecewise smooth and globally $\mathscr{C}^1$-continuous [7]. The finite elements constructed from the class of global $\mathscr{C}^1$-continuous basis functions are referred as $\mathscr{C}^1$-elements. There are limited finite elements which possess $\mathscr{C}^1$-continuity on complex geometries [9]. Thus, an efficient finite element approach to model higher order PDEs with geometric flexibility is required.

Recently, Hughes et al. [7] introduced a new finite element methodology known as the isogeometric analysis (IGA). IGA employs the complex non-uniform rational B-spline (NURBS) based geometry in a finite element analysis application directly, thus obviating the need of link between the computer-aided design and finite element analysis. The advantages of IGA methodology have been demonstrated by a number of publications (see [7] and references there in). In particular, the IGA offers unique advantages in solving problems involving higher-order PDEs such as higher order accuracy, robustness, two- and three- dimensional geometric flexibility, compact support, and $\mathscr{C}^1$ or higher-order continuity. The IGA methodology has been successfully applied to obtain the solutions to a number of important problems (e.g. the higher-order PDEs in [8, 9], among others).

In this paper, we propose the IGA methodology to solve the fourth-order thermo-mechanical PF model. The IGA is capable of representing any arbitrary complex geometry; however as a proof of concept, in this paper we demonstrate the implementation of IGA methodology, particularly to the square-to-rectangular phase transformations on a simple square geometry. In the following sections, we first describe the governing equations and their numerical discretizations, based on the weak form, for implementation in the IGA framework, followed by the numerical experiments.

Mathematical model of the SMA dynamics

SMAs exhibit complex microstructures as a result of different phase transformations [1]. We note that the FePd, InTl materials have cubic-to-tetragonal PTs, where the cubic phase represents the austenite phase and the three tetragonal phases represent martensite variants. The three dimensional mathematical models that describe the 3D phase transformations are highly non-linear and computationally challenging (refer [2, 10]). To make the model tractable, researchers have been using its two-dimensional analog which in this particular case is the square-to-rectangular PT. Here, the square represents the austenite phase and the rectangles represent martensite variants as shown in Fig. 1(a).

The SMAs have temperature dependent microstructure phases. The material exists in the austenite phase above the transition temperature θ_m, while it stabilizes to the martensite phases below θ_m. The austenite and martensite variants could stabilize and co-exist near θ_m. The Landau theory of PTs can be used to characterize the different phases and their PTs, in terms of order parameters (OPs). According to the Landau theory, the free energy of PTs can be defined as a power series in OP. The minima of the free energy correspond to stable or meta-stable phases in SMAs as shown in Fig. 1(b). Now the free energy $\mathscr{F}(\theta, \epsilon)$ for the square-to-rectangular PTs can be defined based on the temperature-dependent Landau energy, as demonstrated by a number of authors [4, 5, 6], is described as

$$\mathscr{F}(\theta, \epsilon) = \frac{a_1}{2}e_1^2 + \frac{a_3}{2}e_3^2 + \frac{a_2}{2}\left(\frac{\theta - \theta_m}{\theta_m}\right)e_2^2 - \frac{a_4}{4}e_2^4 + \frac{a_6}{6}e_2^6 + \frac{k_g}{2}\left[\left(\frac{\partial e_2}{\partial x}\right)^2 + \left(\frac{\partial e_2}{\partial y}\right)^2\right], \quad (1)$$

where a_1, and a_3 are the bulk and shear modulus, a_2, a_4, and a_6 are the Landau constants, k_g is the Ginzburg constant, e_i are the strain components, θ is the material temperature, and θ_m is the transition temperature. The strains components are defined as

$$e_1 = (\epsilon_{xx} + \epsilon_{yy})/\sqrt{2}, \qquad e_2 = (\epsilon_{xx} - \epsilon_{yy})/\sqrt{2}, \qquad e_3 = (\epsilon_{xy} + \epsilon_{yx})/2, \qquad (2)$$

where e_1, e_2, and e_3 are the hydrostatic, deviatoric, and shear strain, respectively and $\epsilon_{ij} = [(\partial u_i/\partial x_j) + (\partial u_j/\partial x_i)]/2$ is the Cauchy-Lagrange strain tensor (with the repeated index convention used); $\boldsymbol{u} = \{u_i\}|_{i=1,2}$ are the displacements along x, and y direction, respectively.

As we are interested in thermo-mechanical properties of SMAs, the governing equations of mechanical and thermal dynamics are derived using the free energy function Eq. 1 [6, 11] as

$$\frac{\partial u_1}{\partial t} = v_1, \qquad (3a)$$

$$\frac{\partial u_2}{\partial t} = v_2, \qquad (3b)$$

$$\rho\frac{\partial v_1}{\partial t} = \frac{\partial \sigma_{11}}{\partial x} + \frac{\partial \sigma_{12}}{\partial y} + \sigma_1^g + \eta\left(\frac{\partial v_1}{\partial x} + \frac{\partial v_1}{\partial y}\right) + f_1, \qquad (3c)$$

$$\rho\frac{\partial v_2}{\partial t} = \frac{\partial \sigma_{21}}{\partial x} + \frac{\partial \sigma_{22}}{\partial y} + \sigma_2^g + \eta\left(\frac{\partial v_2}{\partial x} + \frac{\partial v_2}{\partial y}\right) + f_2, \qquad (3d)$$

$$c_v\frac{\partial \theta}{\partial t} = \kappa\left(\frac{\partial^2\theta}{\partial x^2} + \frac{\partial^2\theta}{\partial y^2}\right) + a_2\frac{\theta}{\theta_m}e_2\frac{\partial e_2}{\partial t} + g, \qquad (3e)$$

where $\boldsymbol{v} = \{v_1, v_2\}$ are the velocity components, $\boldsymbol{\sigma} = \{\sigma_{ij}\}$ $(\sigma_{ij} = \partial\mathscr{F}/\partial\epsilon_{ij})$ is the stress tensor, η is the dissipation coefficient, $\boldsymbol{f} = \{f_1, f_2\}$, are the loads in x and y direction, c_v is the specific heat, κ is the thermal conductivity, and g is the thermal load. The stress tensor components are defined as

$$\sigma_{11} = \frac{1}{\sqrt{2}}\left[a_1e_1 + a_2\left(\frac{\theta - \theta_m}{\theta_m}\right)e_2 - a_4e_2^3 + a_6e_2^5\right], \qquad (4a)$$

$$\sigma_{12} = \frac{1}{2}a_3e_3 = \sigma_{21}, \qquad (4b)$$

$$\sigma_{22} = \frac{1}{\sqrt{2}}\left[a_1e_1 - a_2\left(\frac{\theta - \theta_m}{\theta_m}\right)e_2 + a_4e_2^3 - a_6e_2^5\right], \qquad (4c)$$

and the $\boldsymbol{\sigma}^g = \{\sigma_1^g, \sigma_2^g\}$ are the stress components corresponding to strain gradient terms in the $\mathscr{F}$ [11]. These are the extra stress components corresponding to the domain wall. They are defined as

$$\sigma_1^g = -\frac{k_g}{2}\left[u_{xxxx} + u_{xxyy}\right] + \frac{k_g}{2}\left[v_{xxxy} + v_{xyyy}\right], \qquad (5a)$$

$$\sigma_2^g = +\frac{k_g}{2}\left[u_{xxxy} + u_{xyyy}\right] - \frac{k_g}{2}\left[v_{xxyy} + v_{yyyy}\right]. \qquad (5b)$$

It is observed from the Eqs. 3-5, that the structural and thermal dynamics are intrinsically coupled via temperature θ, strain e_2, and strain rate $\dot{e}_2$ (refer to Eqs. 3e, 4a, and 4c). We convert the governing equations (3) into the non-dimensional form and solve it using the IGA.

Numerical Formulation using the isogeometric analysis

To use the IGA, we first convert the system of the governing equations into the weak form. We discretize the domain using $\mathscr{C}^1$-continuous functions required for the fourth-order PDEs. The generalized-α method is used for time integration along with an adaptive time stepping scheme developed by the authors of [8].

Weak Formulation. Let $\Omega \subset \mathbb{R}^2$ be an open set in the two-dimensional space. The boundary is denoted by Γ and its outward normal by $\boldsymbol{n}$. The weak formulation of the Eqs. 3 is derived by multiplying the equations with weighing functions $\{\boldsymbol{U}, \boldsymbol{V}, \Theta\}$ and transforming them by using the integration by parts. Let X denote both the trial solution and weighting function spaces, which are assumed to be identical. Initially we consider periodic boundary conditions in all directions. Let $(\cdot, \cdot)_\Omega$ denote the L^2 inner product with respect to the domain Ω. The variational formulation is stated as follows:

Find solution $\boldsymbol{S} = \{\boldsymbol{u}, \boldsymbol{v}, \theta\} \in X$ such that $\forall \boldsymbol{W} = \{\boldsymbol{U}, \boldsymbol{V}, \Theta\} \in X$:

$B(\boldsymbol{W}, \boldsymbol{S}) = 0$, with

$$
\begin{aligned}
B(\boldsymbol{W}, \boldsymbol{S}) = {} & \left(\boldsymbol{U}, \frac{\partial \boldsymbol{u}}{\partial t}\right)_\Omega + \left(\boldsymbol{V}, \rho\frac{\partial \boldsymbol{v}}{\partial t}\right)_\Omega + \left(\Theta, c_v\frac{\partial \theta}{\partial t}\right)_\Omega - (\boldsymbol{U}, \boldsymbol{v})_\Omega \\
& + (\nabla\boldsymbol{V}, \boldsymbol{\sigma})_\Omega + (\nabla\boldsymbol{V}, \eta\boldsymbol{v})_\Omega - (\boldsymbol{V}, \boldsymbol{f})_\Omega + (\boldsymbol{V}, \boldsymbol{\sigma}^g)_\Omega \\
& + (\nabla\Theta, \kappa\nabla\theta)_\Omega - (\Theta, g)_\Omega - \left(\Theta, a_2\frac{\theta}{\theta_m}e_2\frac{\partial e_2}{\partial t}\right)_\Omega .
\end{aligned}
\tag{6}
$$

Semi-discrete formulation. The semi-discrete formulation is used for solving the coupled dynamic thermo-mechanical Eqs.6. For the space discretization of Eq. 6, the Galerkin method is used. We approximate Eq. 6 by the following variational problem over the finite element spaces (denoted by superscript h):

Find $\boldsymbol{S}^h = \{\boldsymbol{u}^h, \boldsymbol{v}^h, \theta^h\} \in X^h \subset X$ such that $\forall \boldsymbol{W}^h = \{\boldsymbol{U}^h, \boldsymbol{V}^h, \Theta^h\} \in X^h \subset X$:

$$
B(\boldsymbol{W}^h, \boldsymbol{S}^h) = 0,
\tag{7}
$$

with $\boldsymbol{W}^h$ and $\boldsymbol{S}^h$ defined as

$$
\boldsymbol{W}^h = \{\boldsymbol{U}^h, \boldsymbol{V}^h, \Theta^h\}, \quad \boldsymbol{U}^h = \sum_{A=1}^{n_b} \boldsymbol{U}_A N_A, \quad \boldsymbol{V}^h = \sum_{A=1}^{n_b} \boldsymbol{V}_A N_A, \quad \Theta^h = \sum_{A=1}^{n_b} \Theta_A N_A, \tag{8.1}
$$

$$
\boldsymbol{S}^h = \{\boldsymbol{u}^h, \boldsymbol{v}^h, \theta^h\}, \quad \boldsymbol{u}^h = \sum_{A=1}^{n_b} \boldsymbol{u}_A N_A, \quad \boldsymbol{v}^h = \sum_{A=1}^{n_b} \boldsymbol{v}_A N_A, \quad \theta^h = \sum_{A=1}^{n_b} \theta_A N_A, \tag{8.2}
$$

where N_A's are the basis functions, and n_b is the dimension of the discrete space. The NURBS basis function with $\mathscr{C}^1$-continuity are used.

Numerical experiments - microstructure evolution

In this section, we present the numerical results of microstructure evolution using the developed model. The numerical experiments have been performed on a SMA specimen of $\bar{\Omega} = [0, l] \times [0, h]$. The periodic boundary conditions were applied on all boundaries in both the directions. The FePd material parameters used for the simulations are found in [5]. We consider a square domain with $l = h = 16$ units (in dimensionless form), and employ a uniform mesh composed of $\mathscr{C}^1$-continuous quadratic elements. The structural and thermal initial conditions, used during the microstructure evolution, are $\boldsymbol{u}_0 = x(l-x)y(h-y) \times 10^{-5}$, and $\theta_0 = 250\,\text{K}$, respectively. The simulations have been performed for sufficiently long time by minimizing the energy till it no longer evolves. We compared the stabilized
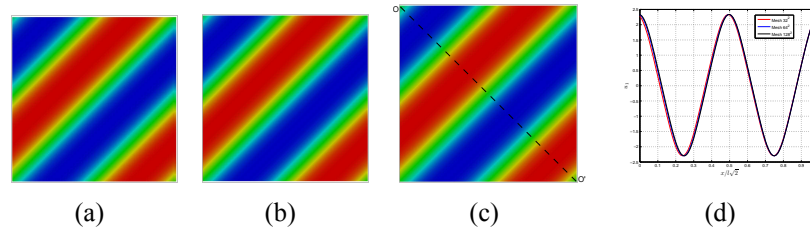
Fig. 2: (Color online) Evolved microstructures e_2 for (a) 32^2, (b) 64^2, and (c) 128^2 mesh refinements. The red and blue colors represent martensite variants ($M+$ and $M-$). The plot (d) shows the variation of u_1 along the cutline O-O' for different meshes.
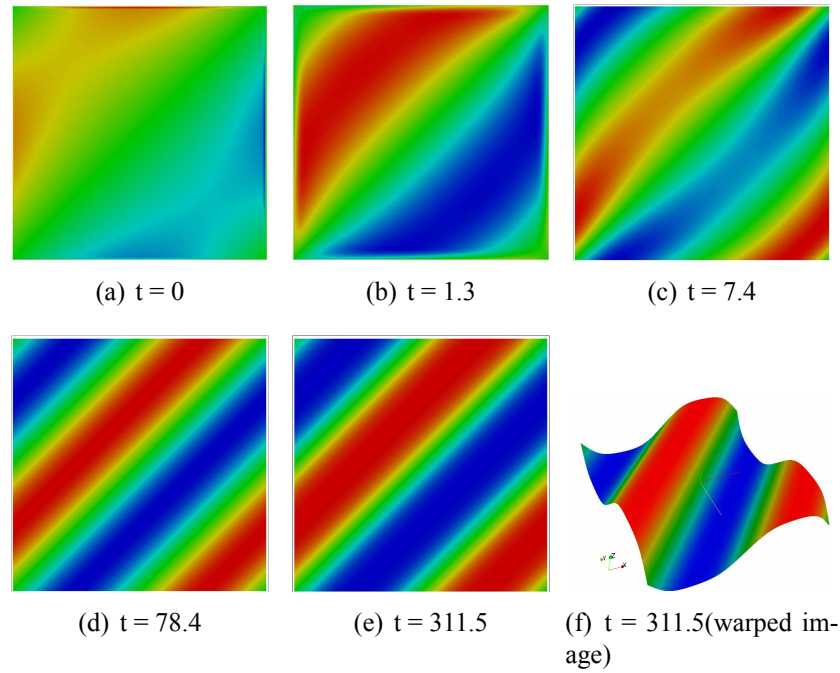

(a) t = 0   (b) t = 1.3   (c) t = 7.4

(d) t = 78.4   (e) t = 311.5   (f) t = 311.5(warped image)

Fig. 3: (Color online) Evolution of microstructures e_2 in time. The plots are rescaled to data range at each time frame for clarity.

solutions using the 32^2, 64^2, and 128^2 mesh refinements. Fig. 2 shows the plot of microstructures for different mesh refinements. We also compared the variation of displacement u_1 along the cutline O-O' (refer Fig. 2(c)) and plotted them for different meshes as shown in Fig. 2(d). We found that the results are practically mesh independent.

Fig. 3 shows the evolution of microstructure at different time frames. It is observed that the domains of martensitic variants ($M+$ and $M-$) are evolved to form microstructures aligned along the diagonal plane. These results are in agreement with the results reported previously [5, 11]. The evolution of the time step size for the adaptive solver during simulations are plotted in Fig. 4(a). We plot the average temperature evolution of the specimen in Fig. 4(b). The temperature increase, observed during the evolution, is the result of the coupling between the structural and thermal equations.

Conclusions

In this paper, the thermo-mechanical phase-field model for SMAs has been solved numerically. More specifically, the IGA framework has been developed for the numerical solution of two dimensional problems focusing on square-to-rectangular phase transformations in SMA materials. We demonstrated the IGA implementation on a square geometry. We have also carried out mesh refinement

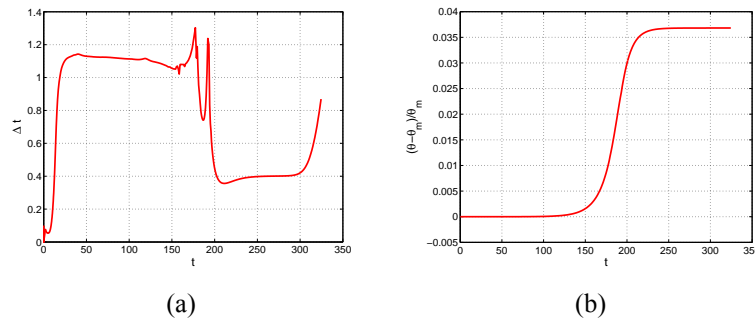(a)   (b)

Fig. 4: Evolution of (a) adaptive time steps, and (b) average rescaled temperature in time.

studies and presented examples of microstructure evolution, which are in agreement with those previously reported in the literature. Results on the IGA implementation on other geometries will be published else-where.

Acknowledgments

References

[1] K. Otsuka and C.Wayman: *Shape memory materials* (Cambridge University Press, New York 1998).

[2] A. Khandelwal and V. Buravalla: Int J of Struct Changes in Solids, Vol. 1, 1 (2011), p. 111

[3] A. Khachaturian: *Theory of structural transformations in solids* (John Wiley & Sons, New York 1983).

[4] R. Melnik, A. Roberts, and K. Thomas: Math Control in Smart Structures, Proc. of SPIE, vol. 3667 (1999), p. 290

[5] M. Bouville and R. Ahluwalia: Acta Mater., Vol. 56, 14,(2008) p. 3558

[6] L. Wang and R. Melnik: Mater. Sci. Eng. A, Vol. 481-482 (2008), p. 190

[7] C.J. Austin, T. Hughes, and Y. Bazilevs: *Isogeometric Analysis: Toward Integration of CAD and FEA* (John Wiley & Sons, 2009).

[8] H. Gomez, V. Calo, Y. Bazilevs, and T. Hughes: Comput Method Appl M, Vol. 197, 49-50 (2008), p. 4333

[9] H. Gomez, T. J. Hughes, X. Nogueira, and V. M. Calo: Comput Method Appl M, Vol. 199, 25-28 (2010), p. 1828

[10] R. Melnik, A. Roberts, and K. Thomas: Comp Mtrl Sci, vol. 18, (2002), p. 255

[11] R. Dhote, R. Melnik, and J. Zu: *Dynamic thermo-mechanical coupling and size effects in finite shape memory alloy nanostructures*, submitted (2012)

State-of-the-Art Research and Application of SMAs Technologies

10.4028/www.scientific.net/AST.78

Phase Field Dynamic Modelling of Shape Memory Alloys Based on Isogeometric Analysis

10.4028/www.scientific.net/AST.78.63

DOI References

[4] R. Melnik,A. Roberts, andK. Thomas: MathControlinSmartStructures, Proc. ofSPIE, vol. 3667(1999), p.290.

http://dx.doi.org/10.1117/12.350084

[6] L. WangandR. Melnik: Mater. Sci. Eng. A, Vol. 481-482(2008), p.190.

http://dx.doi.org/10.1016/j.msea.2006.12.194